



LOW FREQUENCY PLASMA WAVES IN THE SOLAR WIND: FROM ECLIPTIC PLANE TO THE SOLAR POLAR REGIONS

Naiguo Lin*, P. J. Kellogg*, R. J. MacDowall**, E. E. Scime***, J. L. Phillips†, A. Balogh‡ and R. J. Forsyth‡

* School of Physics and Astronomy, University of Minnesota, Minneapolis MN 55455, U.S.A.

** NASA/Goddard Space Flight Center, Greenbelt MD 20771, U.S.A.

*** Physics Department, West Virginia University, Morgantown WV 26506, U.S.A.

† Los Alamos National Laboratory, Los Alamos NM 87545, U.S.A.

‡ Imperial College of Science and Technology, London, U.K.

ABSTRACT

Traveling from the ecliptic to the solar polar regions, Ulysses observed wave activity below the local electron cyclotron frequency, f_{ce} . In regions near the heliospheric current sheet (hereafter HCS regions), two wave modes are observed: (1) whistler mode electromagnetic waves near interplanetary shocks and during periods of rapidly increasing solar wind velocity, and (2) apparently electrostatic waves occurring during the periods when gradually decreasing solar wind velocity is observed. At high heliographic latitudes, in the region with relatively steady high speed solar wind streams, wave activity is consistently observed near and below f_{ce} with little time variability of the spectra. It is found that in the periods when intense waves of the second type are observed in the HCS regions, the electron heat flux decreases. This may imply that these low frequency waves limit the intensity of the heat flux through wave particle scattering.

© 1997 COSPAR. Published by Elsevier Science Ltd.

INTRODUCTION

Low frequency plasma waves ($< f_{ce}$) in the solar wind have been observed and studied previously, mostly within 1 AU from the Sun and near the ecliptic plane (see for example, Gurnett, 1991; Beinroth and Neubauer, 1981). The unique orbit of Ulysses extends our observations into solar polar regions and also to further distances from the Sun. We report here Ulysses observations of low frequency wave activity in the solar wind during 1990 - 1995, as Ulysses completed its first solar polar orbit. The observations cover a radial distance ranging from 1 to 5.5 AU, and heliographic latitudes up to $\pm 80^\circ$, as shown in Figure 1.

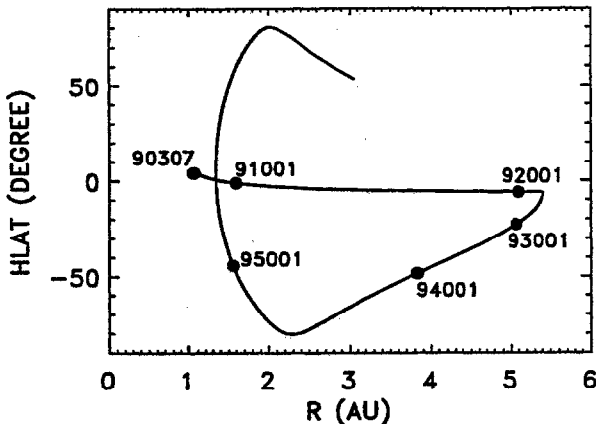


Fig. 1. Ulysses orbit from 1990-1995, plotted in terms of the radial distance from the Sun and the heliographic latitude.

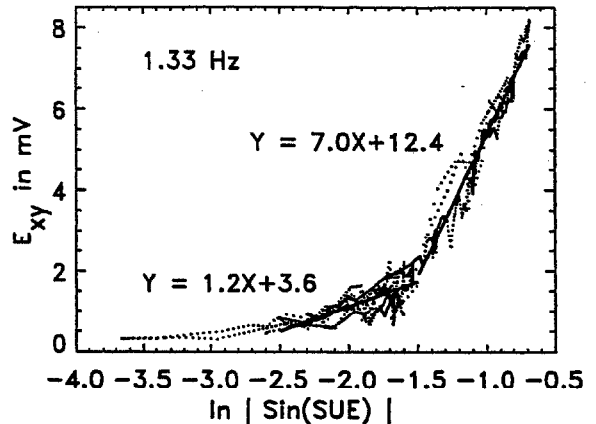


Fig. 2. The 1.33 Hz spin plane electric background plotted vs. logarithm of the sine of SUE angle. The solid lines are the fits to the two parts of the data.

The low frequency plasma wave data are obtained by the waveform analyzer (WFA) which is part of the unified radio and plasma wave (URAP) instrument aboard the Ulysses spacecraft. WFA measures both electric and magnetic fields in 20 channels between 0.22 and 448 Hz (Stone *et al.*, 1992). The data used here are measurements in the spacecraft spin plane with a 64-sec time resolution. The solar wind data (velocity, density, and temperature) are obtained by the plasma wave experiment (SWOOPS). The magnetic field data and the shock list are provided by the magnetometer team.

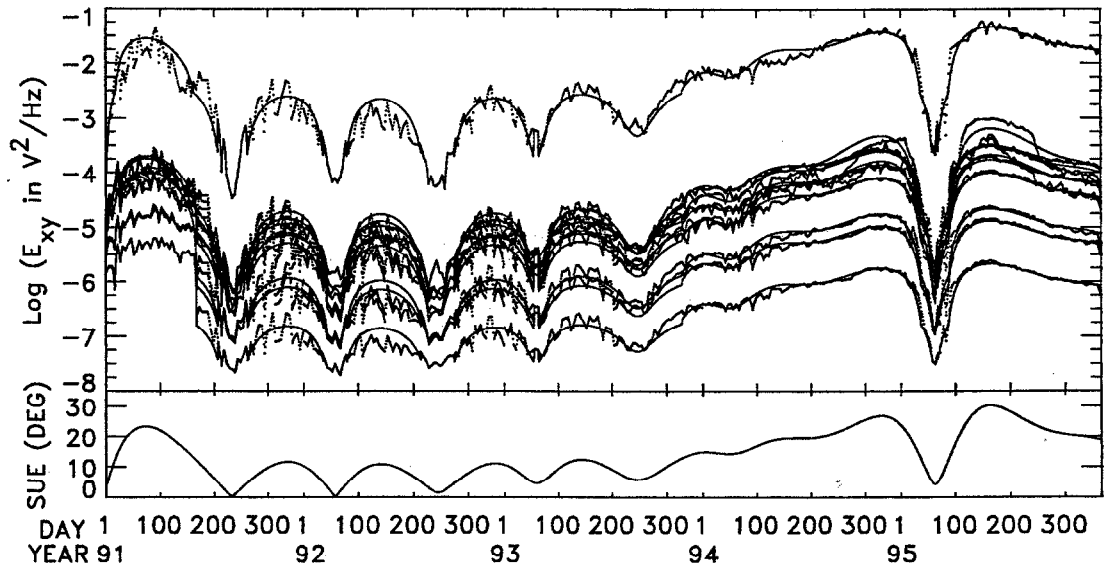


Fig. 3. The background noise of 10 lowband WFA channels derived from data (dotted lines) superimposed with the fit of the background (solid lines) for years 1991 to 1995. Note that the background for the four highest frequency channels before day 168 of 1991 is not fit. The SUE angle is plotted in the bottom panel.

BACKGROUND NOISE DETERMINATION

The URAP instrument has one electric antenna and one magnetic antenna perpendicular to the spin axis. The spin plane electric antenna consists of two monopoles of length 35.2 m each; with a spacecraft diameter of 2.6 m, this gives a tip-to-tip length of 73 m. It is found that the background electric noise of the ten low band channels of WFA (from 0.22 Hz to 5.3 Hz) varies with the solar aspect angle, i.e. the angle between the Sun, Ulysses and the Earth (SUE angle). This variation occurs because of changes in photoelectric emissions as the effective area of the antennas presented to sunlight varies. The effect is similar to that discussed by Kellogg (1980) and Lai *et al.* (1986). The relation between the potential of the antenna, ϕ , and the SUE angle, θ , can be expressed as $e\phi/kT_\phi = \ln|\sin\theta| + C$, where T_ϕ is the photoelectron temperature, and C is a function of some parameters and is assumed to be a constant. Figure 2 shows an example of the relation between the background noise (in millivolts) and $\ln(\sin\theta)$ for the channel with central frequency at 1.33 Hz. The data for $\ln(\sin\theta) \geq -1.5$ ($\theta \geq 12.9^\circ$) and $-2.5 \leq \ln(\sin\theta) < -1.5$ ($4.7^\circ \leq \theta < 12.9^\circ$) are reasonably fit to two straight lines. For $\theta < 4.7^\circ$, the potential becomes nearly constant. Although the background noise for each channel varies with different scan modes of another instrument, the Plasma Frequency Receiver (PFR), and with different bitrates, the above pattern is generally true. For each lowband channel, we have derived background values from the data in every five day period as the average over the 10% of the data with minimum values, and then fit the background with linear relations similar to those in Figure 2. Measurements at fast and slow PFR scan modes, and at two different bitrates are treated separately. The values for $\theta < 4.7^\circ$ are left unchanged. Figure 3 shows the variation of the background noise in years 91-95. The fit values, which are used in this study, are overplotted with solid lines. Detailed discussion on the background determination will be presented in a future paper.

WAVE OBSERVATIONS

Wave activity observed within HCS regions has a different pattern compared to that outside the regions. Within the HCS regions, as Ulysses regularly encountered solar wind turbulence, alternating high and slow speed solar wind streams, and interplanetary shocks, highly variable wave activity is observed in a frequency range from a fraction of hertz up to f_{ce} . These regions are at latitudes equatorward of approximately -40° (heliographic) during the southbound pass and within $\pm 20^\circ$ during the northbound pass.

Figure 4 shows an example of in-ecliptic wave observations. It is clear that the peak power of the wave activity is below f_{ce} (the curve on the spectra). Two kinds of waves are observed: (1) Electromagnetic waves which occur near interplanetary shocks (the vertical dashed lines in the two lower panels) and/or where there is a sharp increase in the solar wind velocity. These waves are usually observed at >10 Hz. The electromagnetic nature of these waves is confirmed by simultaneous observations of magnetic components of the waves (not shown). (2) Waves which occur in expanding solar wind stream regions, i.e. during the intervals when the solar wind velocity is decreasing (horizontal bars in the last panel mark some of such intervals). The maximum frequency of these waves is usually lower than that of the first kind (< 10 Hz), since the ambient magnetic field strength, and thus f_{ce} , is lower during these periods, but they extend to the lowest frequency detectable by the WFA (0.22 Hz). These waves apparently are electrostatic, since there is little magnetic noise detected in these periods. The bottom panel shows variations of the electron heat flux, calculated using the three-dimensional electron spectrometer data (Scime *et al.*, 1994). We notice that when there are intense waves of the second kind, the heat flux level is generally low, while near shocks the heat flux level is much higher.

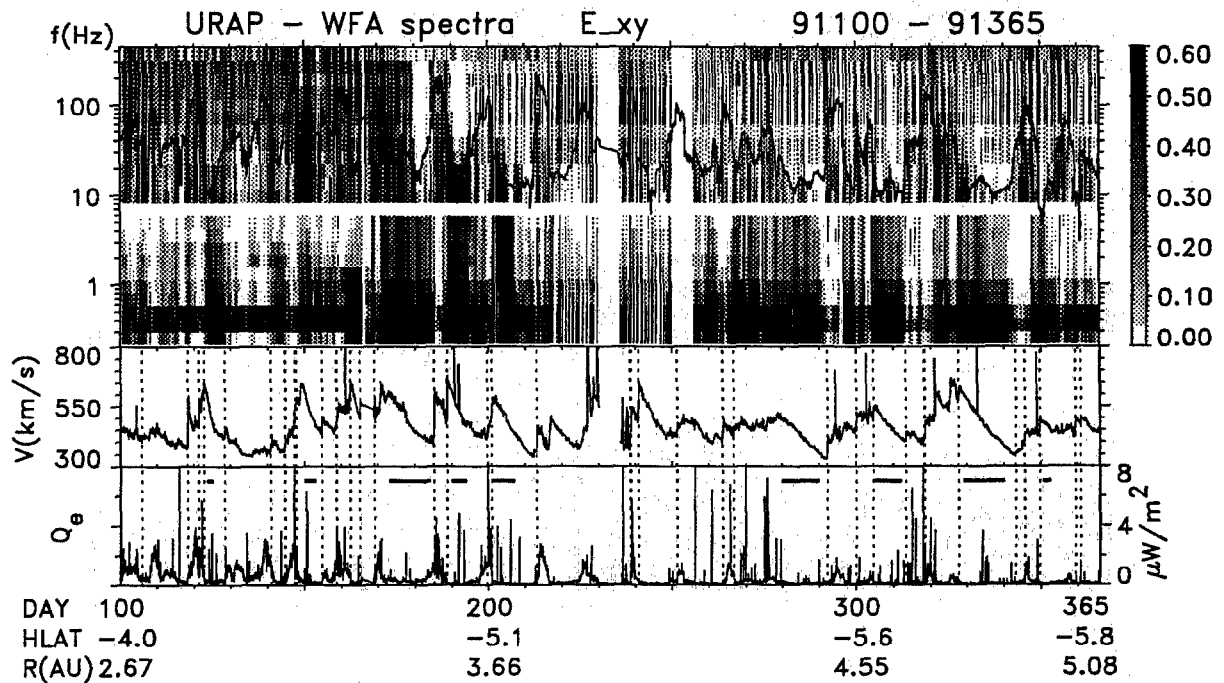


Fig. 4. Top: Dynamic spectra of the relative intensity (Log (data-background)/background) of one-hour averaged electric wave power measured in the spacecraft spin plane in the frequency from 0.2 to 448 Hz for the period from day 100 to day 365 of 1991. The local electron cyclotron frequency is overplotted with a curve. The vertical stripes crossing all channels are data gaps. Middle: The solar wind velocity. The times when interplanetary shocks were observed are marked with vertical dashed lines. Bottom: The electron heat flux. Horizontal bars in the panel indicate the intervals when electrostatic waves are observed.

Figure 5 shows electric wave spectra (top panel) observed during the northbound "fast latitude scan" in 1995. It shows that as soon as *Ulysses* entered the HCS region (on about day 35, -20° latitude), alternating occurrences of the two kinds of waves similar to those in Figure 4 were observed. This feature disappears after *Ulysses* went out of the region (on about day 90, $+20^\circ$). The periods of decreasing solar wind velocity when the second type of waves are observed are marked with horizontal bars in the velocity panel. The bottom panel displays the spectra of spin plane magnetic signals. Within the HCS region, corresponding to the > 10 Hz electric waves, strong magnetic waves are observed near shocks or where there is a sharp increase in the solar wind velocity, while in the marked intervals, magnetic signals are usually not detected. The time variation of electron heat flux (the third panel) again shows that the second type of waves is associated with the low level heat flux, while the electromagnetic waves are associated with much higher heat flux.

At high latitudes, outside the HCS region, where the solar wind has a relatively constant speed and the solar wind magnetic field becomes relatively stable, the wave spectra become structureless: wave activity

is constantly observed below f_{ce} , and little electric wave below 10 Hz is observed. In Figure 5, the periods before day 35 and after day 90 exhibit such high latitude wave features (see also, Stone *et al.*, 1995; MacDowall *et al.*, 1996). The nature of these waves will be studied in a future work.

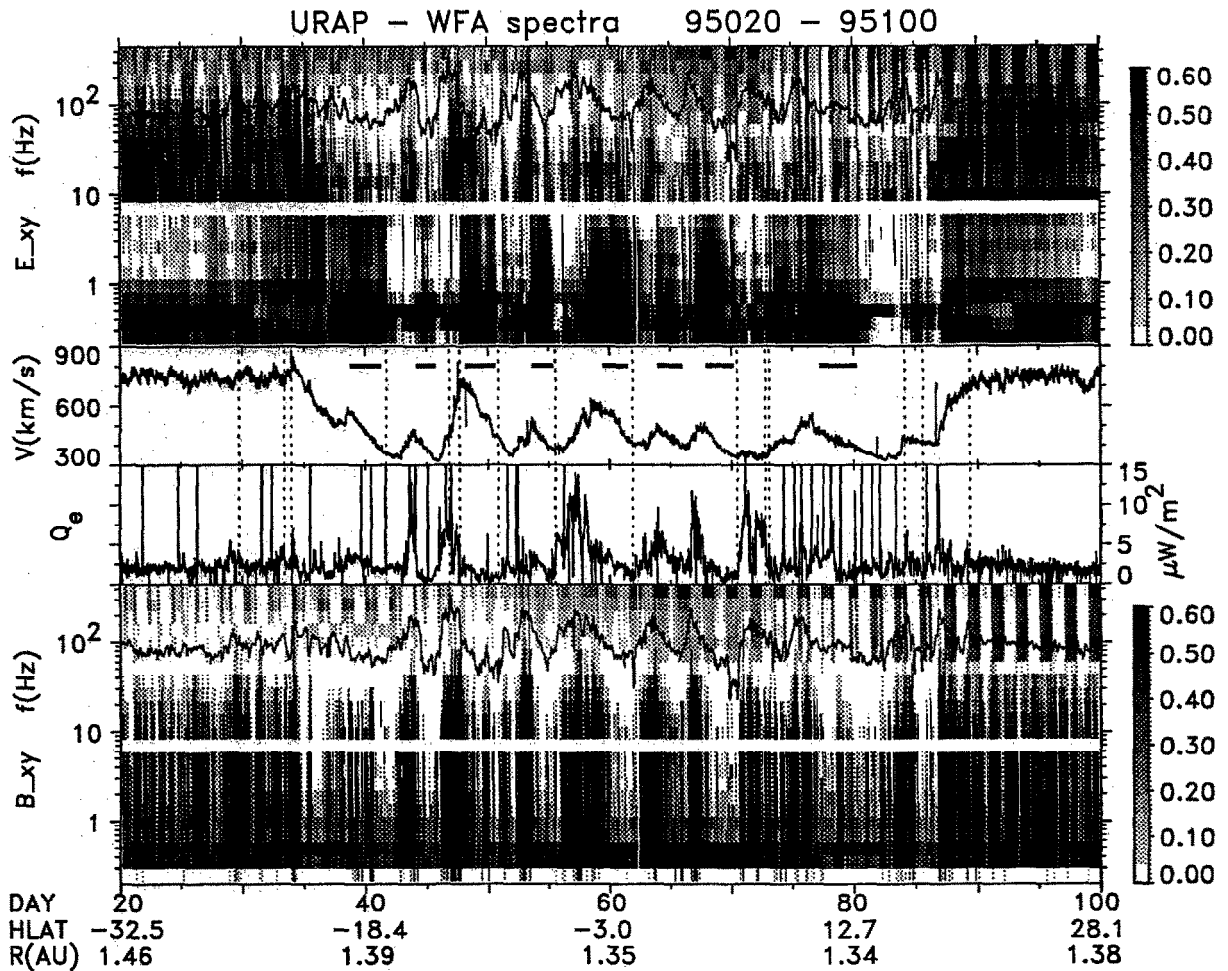


Fig. 5. Top: Electric wave power for the period from day 20 to day 100 of 1995, plotted in the same format as that in Figure 4. Middle: The solar wind velocity and the electron heat flux. The vertical dashed lines mark shock and HCS crossings. Bottom: Magnetic wave power in the same format as that of the electric spectra.

DISCUSSION

The electromagnetic waves observed near interplanetary shocks are believed to be whistler mode which has been studied extensively in the past (for example, Neubauer *et al.*, 1977; Lengyel-Frey *et al.*, 1994). Electron cyclotron resonance is the most likely mechanism for their excitation, with electron temperature anisotropy $T_{\perp} > T_{\parallel}$ as the free energy source. Using recent Ulysses data, Pierre *et al.* (1995) showed that downstream of a shock, the anisotropy increased to above a critical value when the waves were observed. The existence of a marginally stable state may allow waves to propagate far away from their emission points.

The second kind of waves has not been reported before. The low intensity of electron heat flux when these waves occur may imply that the waves have limited the intensity of the heat flux through wave particle scattering. It has been proposed (Gary *et al.*, 1994, and references therein) that the electron heat flux may excite some instabilities and the wave particle scattering by the resulting fluctuations can limit the heat flux. Among them, the whistler heat flux instability may excite waves at the observed frequencies. But the instability has a maximum growth rate in the direction parallel to the background magnetic field and produces primarily magnetic fluctuations (Gary *et al.*, 1994). This seems to contradict our observations

of the waves being electrostatic. One possibility is that the waves propagate obliquely near the resonance cone and so have a large E/B ratio. Marsch and Chang (1982) have suggested that in a typical solar wind plasma "hybrid" whistler modes can be excited with the free energy provided by resonant halo electrons. These waves propagate at large oblique angles and become nearly electrostatic. The cutoff frequency of these electrostatic modes is near the lower hybrid frequency, which, in our case, is near the lowest frequency that can be detected by the WFA instrument. More detailed work is needed to determine the propagation angle and other properties of the observed waves. Comparison of the previous theories with the observed conditions of the solar wind plasma when these electrostatic noise are observed may provide new insight into the generation mechanism of these waves and the source of heat flux regulation in the solar wind.

ACKNOWLEDGMENTS

NL thanks S. P. Gary for helpful discussions and D. Thayer of the University of Minnesota for assistance in data processing. The URAP experiment is a collaboration of NASA/Goddard Space Flight Center, the Observatoire de Paris-Meudon, the University of Minnesota, and the Centre des Etudes Terrestres et Planetaires, Velizy, France. The work at Los Alamos was carried out under the auspices of the U.S. Department of Energy with support from NASA.

REFERENCES

- Beinroth, H. J., and F. M. Neubauer, *J. Geophys. Res.*, **86**, 7755 (1981).
 Gary, S. P., E. E. Scime, J. L. Phillips, and W. C. Feldman, *J. Geophys. Res.*, **99**, 23391 (1994).
 Gurnett, D. A., in *Physics of the Inner Heliosphere*, eds. R. Schwenn and E. Marsch, pp. 135-157, Springer-Verlag, Berlin (1991).
 Kellogg, P. J., *J. Geophys. Res.*, **85**, 5157 (1980).
 Lai, S. T., H. A. Cohen, T. L. Aggson, W. J. McNeil, *J. Geophys. Res.*, **91**, 12137 (1986).
 Lengyel-Frey, D., W. M. Farrell, R. G. Stone, A. Balogh, and R. Forsyth, *J. Geophys. Res.*, **99**, 13325 (1994).
 MacDowall, R. J., *et al.*, *Astron. Astrophys.*, **316**, 396 (1996).
 Marsch, E., and T. Chang, *Geophys. Res. Lett.*, **9**, 1155 (1995).
 Neubauer, F. M., G. Musmann, and G. Dehmel, *J. Geophys. Res.*, **82**, 3201 (1977).
 Pierre, F., *et al.*, *Geophys. Res. Lett.*, **22**, 3425 (1995).
 Scime, E. E., S. J. Bame, W. C. Feldman, S. P. Gary, and J. L. Phillips, *J. Geophys. Res.*, **99**, 23401 (1994).
 Stone, R. G. *et al.*, *Astron. Astrophys. Supp. Ser.*, **92**, 291 (1992).
 Stone, R. G. *et al.*, *Science*, **268**, 1026 (1995).